5-1-2019

Morphology evolution of Janus dumbbell nanoparticles in seeded emulsion polymerization

Yifan Li
Iowa State University, yifanli@iastate.edu

Shensheng Chen
Binghamton University--SUNY

Serkan Demirci
Iowa State University

Shiyi Qin
Binghamton University--SUNY

Zihao Xu
Iowa State University, zihaoxu@iastate.edu

See next page for additional authors

Morphology evolution of Janus dumbbell nanoparticles in seeded emulsion polymerization

Abstract

Emulsion polymerization is a versatile approach to produce different polymeric nanoparticle morphologies, which can be useful in a variety of applications. However, the detailed mechanism of the morphology formation is not entirely clear. We study the kinetics of nanoparticle morphology evolution during a seeded emulsion polymerization using both experimental and computational tools. Lightly crosslinked polystyrene seeds were first synthesized using dispersion polymerization. Then the seed particles were swollen in tert-butyl acrylate and styrene monomers, and subsequently polymerized into nanoparticles of dumbbell and multilobe morphologies. It was discovered that both the seed and final particle morphology were affected by the methanol concentration during the seed synthesis. Systematically adjusting the methanol amount will not only yield spherical seed particles of different size, but also dumbbell particles even without the second monomer polymerization. In addition to methanol concentration, morphology can be controlled by crosslinking density. The kinetics studies revealed an interesting transition from multilobe to dumbbell geometries during the secondary polymerization. Based on the results, a nucleation-growth model has been proposed to describe the morphology evolution and verification was offered by computer simulation. The key discovery is that nanoparticle morphology can be kinetically controlled by diffusion of the protrusions on the seed particles. The condition of seed synthesis and crosslinking density will drastically change the seed and final nanoparticle morphology.

Keywords

Polymeric nanoparticles, Janus particles, Emulsion polymerization, Dispersion polymerization

Disciplines

Materials Chemistry | Materials Science and Engineering | Nanoscience and Nanotechnology | Polymer and Organic Materials

Comments

This is a manuscript of an article published as Li, Yifan, Shensheng Chen, Serkan Demirci, Shiyi Qin, Zihao Xu, Emily Olson, Fei Liu, Devin Palm, Xin Yong, and Shan Jiang. "Morphology evolution of Janus dumbbell nanoparticles in seeded emulsion polymerization." *Journal of Colloid and Interface Science* 543 (2019): 34-42. DOI: 10.1016/j.jcis.2019.01.109. Posted with permission.

Authors

Yifan Li, Shensheng Chen, Serkan Demirci, Shiyi Qin, Zihao Xu, Emily Olson, Fei Liu, Devin Palm, Xin Yong, and Shan Jiang

Morphology evolution of Janus dumbbell nanoparticles in seeded emulsion polymerization

Yifan Li [a,1], Shensheng Chen [b,1], Serkan Demirci [a], Shiyi Qin [b], Zihao Xu [a], Emily Olson [a], Fei Liu [a], Devin Palm [a], Xin Yong *[b] and Shan Jiang *[ac]

[a]Department of Materials Science and Engineering, Iowa State University of Science and Technology, Ames, IA 50011, USA. E-mail: sjiang1@iastate.edu

[b]Department of Mechanical Engineering, Binghamton University, Binghamton, NY 13902, USA. E-mail: xyong@binghamton.edu

[c]Division of Materials Science & Engineering, Ames National Laboratory, Ames, IA 50011, USA

*Corresponding author.

E-mail address: sjiang1@iastate.edu (S. Jiang), xyong@binghamton.edu (X. Yong)

[1] Equal contribution and co-first author.

Abstract

Emulsion polymerization is a versatile approach to produce different polymeric nanoparticle morphologies, which can be useful in a variety of applications. However, the detailed mechanism of the morphology formation is not entirely clear. We study the kinetics of nanoparticle morphology evolution during a seeded emulsion polymerization using both experimental and computational tools. Lightly crosslinked polystyrene seeds were first synthesized using dispersion polymerization. Then the seed particles were swollen in tert-butyl acrylate and styrene monomers, and subsequently polymerized into nanoparticles of dumbbell and multilobe morphologies. It was discovered that both the seed and final particle morphology were affected by the methanol concentration during the seed synthesis. Systematically adjusting the methanol amount will not only yield spherical seed particles of different size, but also dumbbell particles even without the second monomer polymerization. In addition to methanol concentration, morphology can be controlled by crosslinking density. The kinetics studies revealed an

interesting transition from multilobe to dumbbell geometries during the secondary polymerization. Based on the results, a nucleation-growth model has been proposed to describe the morphology evolution and verification was offered by computer simulation. The key discovery is that nanoparticle morphology can be kinetically controlled by diffusion of the protrusions on the seed particles. The condition of seed synthesis and crosslinking density will drastically change the seed and final nanoparticle morphology.

1. Introduction

Emulsion polymers are widely used in industry applications including low VOC (volatile organic compound) waterborne coatings, personal and home care products, and construction chemicals [1, 2]. Major efforts have been focused upon control of the chemical composition and particle size of the polymer [3-8]. In recent years, significant attention has been given to the morphology control of colloids using seeded emulsion polymerization [7-9]. By adjusting the reaction condition, the combination of seed and monomer chemistry, and feeding sequence, various morphologies such as core-shell, multilobe, raspberry and dumbbell can be produced [10-14]. These unique particle morphologies have been proven to be useful for industry applications. For example, multilobe morphology was utilized in industry for improving the coating rheology [15]. Another important morphology is the asymmetric dumbbell shape, which has shown promising results in the area of Janus particle research. Janus particles have different chemical compositions on the two sides of a single particle. The anisotropic characteristic of these particles enables the formation of fascinating self-assembly structures [16], which show applicability in emulsion stabilization [17-20], microreactor catalysis [21], multi-functional coatings [22] and drug delivery [23]. However, conventional methodologies for particle synthesis limited the yield capabilities [24]. Through emulsion polymerization, several research groups have produced polymeric Janus dumbbell particles in large quantities [25-30]. This alternative fabrication method produces particles with excellent qualities and consistent morphologies [11, 26, 31, 32].

Despite previous successes, it is still very challenging to predict particle morphology in a seeded emulsion polymerization. It was observed that reaction conditions including stirring speed, temperature, pH,

concentration, and feeding speed and sequence, may drastically change the final particle morphology [28, 33, 34]. In many cases, monomer choice and crosslinking density are also critical to the final particle morphology [35]. Although the basic thermodynamics of the dumbbell formation has been analyzed and partially verified through prior experiments [36, 37], there is not a general principle to follow for morphology control. More importantly, most efforts have reported different particle morphologies through a trial-and-error approach, while the mechanism and morphology evolution remain unclear. In order to provide a deeper understanding of the seeded emulsion polymerization and morphology formation, we studied a simple system using polystyrene particles as the seed and tert-butyl acrylate as the second monomer [12, 38]. The kinetics of the morphology evolution were monitored using electron microscopy. We systematically varied the solvent composition by adjusting the methanol-water ratio and discovered that this ratio drastically changed both seed and final particle morphology. A dumbbell seed geometry was obtained even prior to the second monomer polymerization for the first time. In addition, it was found that the dumbbell morphology can be formed through the merging of distributed lobes on a single seed particle during the secondary polymerization. Furthermore, increasing the crosslinker amount during the second monomer polymerization induces a morphology transition of the final Janus particle from dumbbell to multilobe.

The intricate interplay between kinetics, thermodynamics, and molecular transport in multistage emulsion polymerization poses the biggest challenge to experimental investigation. On the other hand, computer simulation can readily isolate and elucidate competing effects, make it an indispensable tool for establishing a clear reaction–morphology relationship. Various models [39-43] can predict equilibrium particle morphologies based on molecular thermodynamics. However, these equilibrium models do not provide any dynamic information and cannot reveal morphology formation. Although nonequilibrium simulations [44-49] have been developed to capture the detailed polymerization kinetics and spatialtemporal evolution of particle morphology, no dynamic model considers the transport of entangled polymer chains during the reaction. A novel coarse-grained simulation was established in this study to

probe the morphology evolution in the secondary polymerization. Using a mesoscale representation of polymer chains and monomers, this model bridges the disparate length scales between individual polymer coils and the whole particle. More importantly, the dynamics of entangled polymers were captured to elucidate the effect of topological constraints on the morphology development of crosslinked particles. Our simulation was able to reproduce the morphology transition from multilobe to dumbbell and provides unique insight into the kinetics of multistage emulsion polymerization. Based on the experimental and computational evidence, we propose a nucleation-growth kinetic model for the morphology change and dumbbell formation.

2. Experimental

2.1. Materials

Styrene (St, 99%), tert-Butyl Acrylate (tBA, 99%), toluene (99.5%), divinylbenzene (DVB, 99%), polyvinylpyrrolidone (PVP, Mn = 29 000 g mol^{-1}), methanol (MeOH, anhydrous, ~99.5%), poly(vinyl alcohol) (PVA, Mw = 13 000-23 000 g mol^{-1}, 87-89% hydrolyzed) and 2,2′-Azobis(isobutyronitrile) (AIBN, 98%) were purchased from Sigma-Aldrich (USA). St, tBA were distilled under reduced pressure before use. The other chemicals were used as received. Deionized double distilled water was used in all experiments.

2.2. Preparation of polystyrene seed

The seeded emulsion polymerization is known to be a two-step process. First, the seed particles are synthesized by dispersion or emulsion polymerization. Second, the seed particles are swollen by a monomer where the protrusions emerge on the seed particle surface, and subsequently polymerized into the final particle morphology. For the seed synthesis, crosslinked polystyrene nanospheres were prepared by dispersion polymerization. Typically, in a 250 mL round-bottom flask, 3 g PVP was dissolved in a methanol-water mixture with a total weight of 31g under mechanical stirring. In this step, the solvent solubility is adjusted via alteration of the weight fraction of methanol from 50% to 85%. 1.6 g styrene and 0.025g AIBN was then added into the flask. The solution was deoxygenated by bubbling nitrogen for 15

min. The flask was then placed in an oil bath at 55 ± 1 °C and 100 rpm of mechanical stirring rate was applied. After polymerization for 1.5 h. 0.8 g styrene and 55 µL DVB dissolved in 11 g solvent was slowly added into the flask within 2 h. The milky dispersion of crosslinked polystyrene nanospheres was cooled under room temperature and then washed and separated by centrifugation at 14000 rpm in the methanol-water mixture for three times. The crosslinked polystyrene nanospheres were redispersed in 1% PVA aqueous solution for the next step.

2.3. Synthesis of polystyrene/tert-butyl acrylate nanoparticles

Preparation of the final nanoparticles was performed by using a modified seeded polymerization method and crosslinked polystyrene nanospheres as seeds. Typically, a 0.5 mL dispersion of crosslinked polystyrene nanospheres (25 wt.%) in a 1 wt% PVA aqueous solution was mixed with a 1.0 mL emulsion of monomer (20 vol.%). The monomer emulsion consisted of monomer (20 vol%), DVB (0-2 wt.%), and AIBN (0.5 wt%) in a 1 wt% PVA aqueous solution. The mixture was stirred for 0.5 h with a speed of 100 rpm at room temperature to allow the crosslinked polystyrene nanospheres to completely swell. Then, the mixture was deoxygenated by bubbling nitrogen for 2 min. Polymerization was performed by stirring again for 5 h at 70 ± 1 °C in an oil bath. After that, the particles were washed thoroughly in methanol by centrifugation at 14000 rpm for three times.

2.4. Characterization

The morphology of anisotropic Janus particles was investigated by scanning electron microscopy operated at 10 kV (FEI Quanta-250 SEM, USA). To prepare samples for the SEM study, a drop of particle dispersion was diluted with deionized water to obtain a translucent suspension and ultrasonicated for 5 min. Then, the samples were prepared by placing a drop of diluted dispersion on a conductive silicon wafer and allowing the solvent to evaporate at room temperature. The samples were then sputter-coated with a layer of gold (Au) of about 2 nm.

To image the particle morphology during the swelling and polymerization processes, samples were aliquoted from the reaction mixture at different time intervals during the process. Morphology observation was conducted by SEM. Typically, 1 mL of resultant emulsion was taken out and centrifuged at 14000 rpm for 8 min to sediment the particles, and the supernatant was discarded. The particles were redispersed using ultrasonication into 5 g of deionized water. This procedure was repeated two more times to remove surfactant and unreacted monomers.

The size and size distribution of spherical polystyrene seeds were studied by dynamic light scattering (Zetasizer Nano ZS, Malvern Panalytical Ltd). Prior to conducting the measurement, polystyrene seed dispersions were highly diluted and then introduced into a thermostated scattering cell at 25 °C.

The glass transition temperature (T_g) of polystyrene seeds was evaluated with a differential scanning calorimetry instrument (DSC Q2000, TA Instruments, USA) at a rate of 10°C/min in the range of 25°C to 150°C under nitrogen atmosphere. During DSC analysis, about 5 mg of sample was used. At least 3 replicates were measured to obtain the standard deviation.

2.5. Computational model

We performed dynamic modeling of morphology evolution in the second monomer polymerization using dissipative particle dynamics (DPD) [50-52]. DPD models multicomponent systems on the mesoscale by representing a fluidic element as individual coarse-grained beads, whose dynamics are governed by classical mechanics. An advantage of DPD over atomistic molecular dynamics involves the ability to probe physical phenomena occurring at relatively large length and time scales within computationally reasonable time frames, which makes it particularly suitable for simulating polymeric systems [53-55]. Herein, individual polymer chain or a cluster of monomers was represented as one DPD bead [47-49]. The Gibbs free energies of mixing between seed polymer, second monomer, and second polymer as well as the interfacial tensions between domains rich in different components were controlled by DPD

interactions cross differing types of beads [52]. Crosslinking of polymers was modeled by forming permanent bonds between polymer beads and tetrafunctional crosslinkers. The crosslinking in the simulation represents the formation of network, which effectively include both physical crosslinking of chains themselves and chemical crosslinking in the presence of crosslinkers. Polymerization was simulated by simple conversion of bead types from monomer to polymer. Induced by polymerization, the seed polymers and the second polymers underwent phase separation, which resulted in particle morphology evolution.

Entanglement effects between the seed and secondary polymer networks is expected to significantly influence the viscoelastic and dynamics of protrusions. Therefore, we introduced dynamic bonds between the two networks to qualitatively capture polymer entanglements. These bonds formed and broke according to the Bell model [56-58]. The details of DPD method, polymerization and crosslinking reactions, and entanglement models are described in SI. The morphology development and particle formation kinetics were investigated by varying the degrees of crosslinking in the seed particle and in the second polymers. Notably, the numerical degree of crosslinking in the model is defined as the fraction of polymer beads that establish permanent bonds with two crosslinkers (also see SI for additional discussion of the computational crosslinking degree). Thus, this quantity characterizes only the extent of network formation and is different from the crosslinking density or the crosslinker concentration referred to in our experiments.

3. Results and discussion

The various morphologies formed at the expense of methanol-water ratio and stage of seeded emulsion polymerization are depicted in **Fig. 1**. The morphology changes are initiated during the swelling stage, and it is found that distinct ratio of methanol-water will lead to different morphologies of seed particles. Two prominent morphologies were formed via the change in solvent ratio: dumbbell and multilobe. Interestingly, multilobe morphology in the swelling stage does not always lead to multilobe formation in the final particle morphology. It was found that seed particles produced with an intermediate methanol-

water (3:1) ratio can swell into multilobe morphology. These multilobe geometries can transition into dumbbells following a secondary monomer polymerization. This transition is solely dependent upon the methanol-water ratio, with all other experimental conditions kept consistent. In the following text, we will discuss the details of seed morphology and the influence of crosslinker amount on the morphology change.

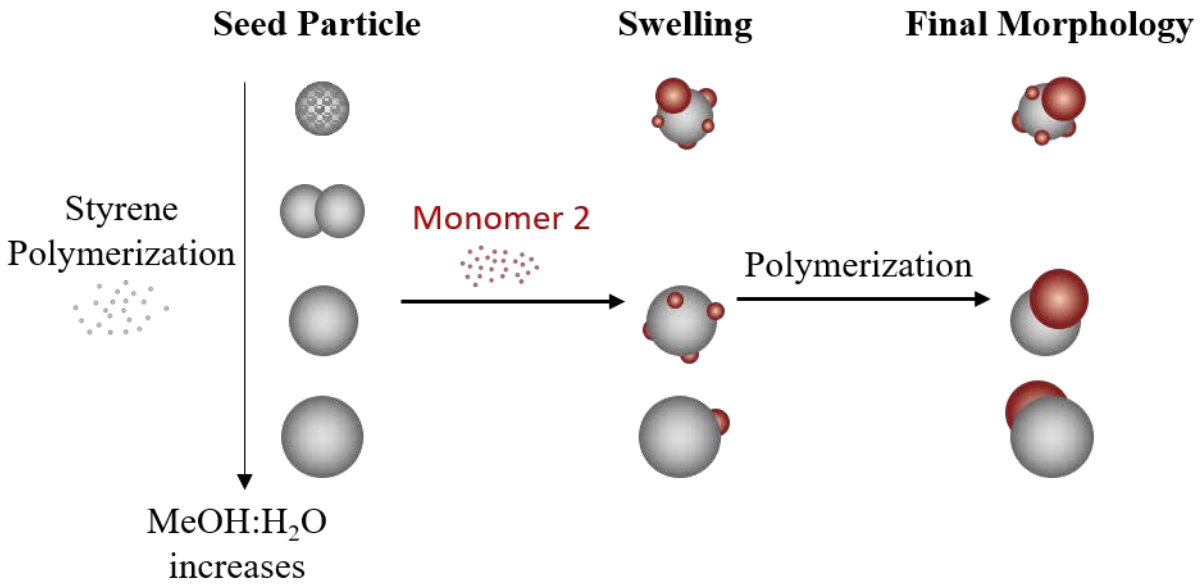

Fig. 1. Schematic illustration of morphology evolution during the seeded emulsion polymerization.

3.1. Seed morphology

To form the seed, linear polystyrene was first synthesized, which showed a milky white appearance after polymerization was triggered by raising temperature to 70°C. Then a small amount of styrene monomer was titrated slowly into the reaction together with crosslinker divinylbenzene (DVB). Titration of the crosslinker following the initial seed formation is a simple practice in dispersion polymerization to ensure seed uniformity and narrow size distribution, which has been reported in literature [11]. Here, the solubility of styrene monomer in the solvent mixture of methanol and water plays an important role. Initially styrene is fully dissolved. As the polymerization progresses, the polystyrene chains grow longer and begin to precipitate out from the solution. The initial precipitation provides nucleation sites for further

polymer aggregation and particle growth, and this procedure inherently forms spherical colloidal particles. When the methanol-water ratio increases, the precipitation occurs at larger polystyrene molecular weights, which has been confirmed by gel permeation chromatography (GPC) (Table S1). In addition to enhanced molecular weight, particle size also increases as the methanol-water ratio increases. Each spherical polystyrene seed has a narrow size distribution, as indicated by dynamic light scattering (DLS) measurement (**Fig. S1**). More importantly, it is noted that the morphology also changes as the methanol-water ratio increases (**Fig. 2**). At 1:1 methanol-water ratios, seed particles adopt a spherical shape with rough surfaces. The rough surface resembles the polystyrene surface with higher crosslinking density [59, 60]. As the methanol-water ratio increases, the seed surface becomes smoother.

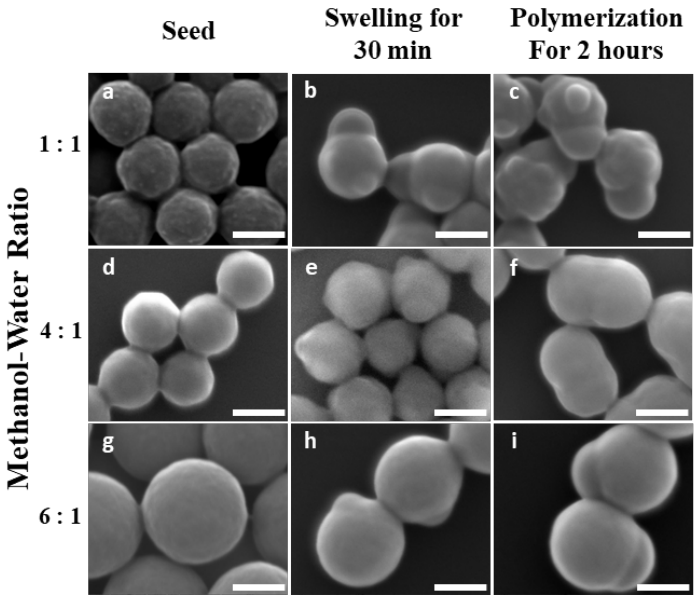

Fig. 2. SEM images of particle morphology evolution during a seeded emulsion polymerization: (a-c) seed synthesized with methanol-water 1:1; (d-f) seed synthesized with methanol-water 4:1; (g-i) seed synthesized with methanol-water 6:1. Scale bar is 200 nm.

More interestingly, at 3:1 methanol-water ratio, the seed particles undergo a transition to a dumbbell morphology even before the second monomer polymerization. As shown in **Fig. 3**, the dumbbell morphology can be further modulated by adjusting the amount of styrene monomer titrated together with

the crosslinker. The detailed mechanism of dumbbell formation in seed particle synthesis is out of the scope of this study. However, it may be due to the stability of seed particles during the polymerization, which is closely related to the methanol-water ratio.

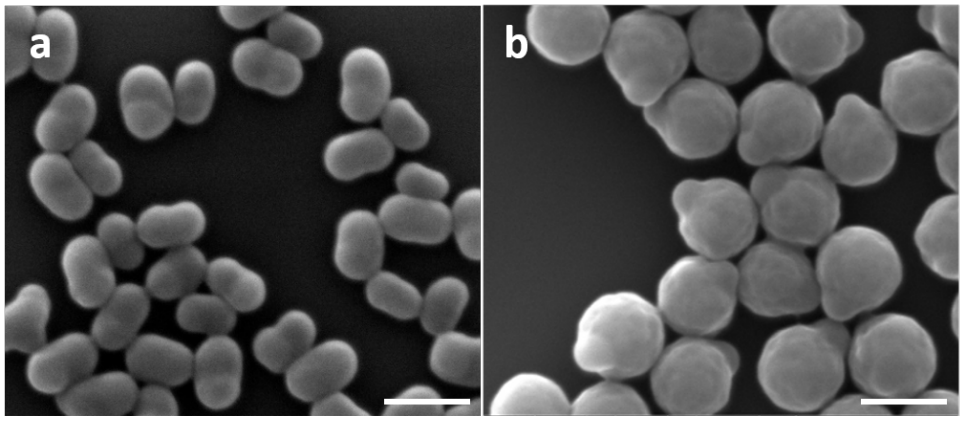

Fig. 3. SEM images of anisotropic dumbbell shape polystyrene seed particles (a) low styrene concentration during titration; (b) high styrene concentration during titration. Scale bar is 500 nm.

In previous studies, it has been observed that highly crosslinked polystyrene particles have rougher surfaces and would lead to multilobe morphology. [11, 59-61]. In order to determine the difference in crosslinking density among all the polystyrene seeds, the glass transition temperature following the addition of crosslinker was measured by DSC. The data (**Fig. S2 and Table S1**) clearly shows that the T_g of the seed particle decreases as methanol-water ratio increases. T_g is correlated with two factors in this system: molecular weight and crosslinking density. Previous results show that increasing methanol-water ratio increases, average molecular weight increases, which should lead to higher T_g. Therefore, the lower T_g measured by DSC can only be explained by the lower crosslinking density. Indeed, as more methanol is added to the reaction, particle size grows and surface roughness decreases, which is a good indication of a decreasing degree of crosslinking density. This can be explained by considering the distribution of crosslinker DVB molecules in the system. At low methanol-water ratio, DVB molecules are less soluble in the solvent and prefer to accumulate more in the seed particles, therefore higher crosslinking densities can be accomplished in seed particles. As the methanol amount increases, DVB molecules may distribute

more in the solvent and the concentration in seed particles decreases. Thus, the crosslinking density of seed particles decreases as the methanol- water ratio increases.

3.2. Swelling morphology and final particle morphology

When swollen with second monomers, the seed particles synthesized with different methanol-water ratios showed very different morphologies. When methanol content is low in seed synthesis (1:1 ratio), the seed particles are swollen into multilobe morphology. Many particles also form one dominant lobe together with several smaller lobes. Such features can be clearly seen under SEM (**Fig. S3**). After polymerization of the second monomer, the lobes all grow into bigger lobes and the final morphology is multilobe. As shown in **Fig. S4**, multiple images from different areas indicate that the observed local morphology is consistent throughout the samples. When the methanol-water ratio increases to 4:1, the seed particles again are swollen into multilobes. However, after polymerization of the second monomer, the morphology evolves into dumbbell shape. The detailed kinetics of multilobe to dumbbell transition are captured in **Fig. 4**.

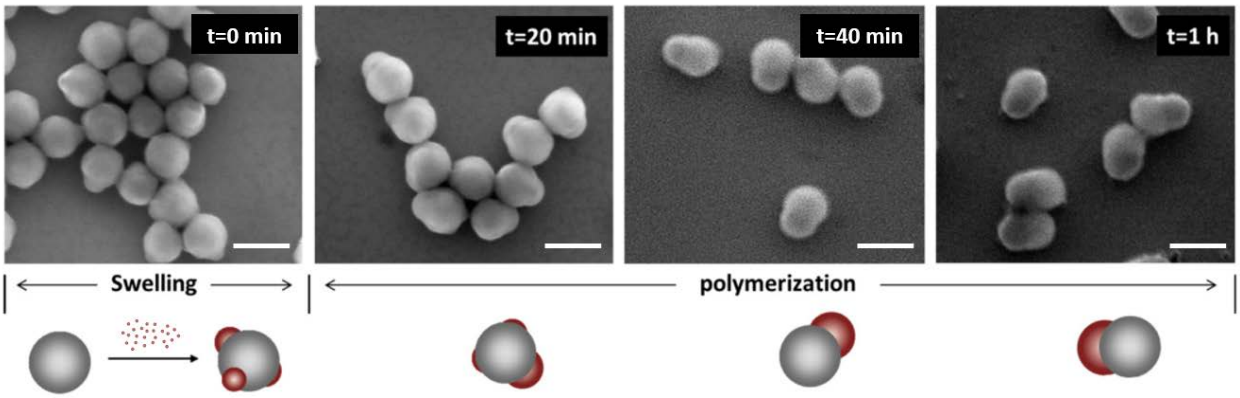

Fig. 4. Morphology transition from multilobes to a single protrusion during the polymerization with seed synthesized under 4:1 methanol-water ratio. Scale bar: 500 nm.

The figure shows that 20 min into the polymerization, one dominant lobe starts to emerge on the seed particle surface. Gradually the smaller lobes all disappear, and the particles eventually morph into a dumbbell shape at 40 min. As polymerization further progresses, the lobe on the dumbbell continues to

grow. This multilobe to dumbbell transition reveals interesting mechanisms of the dumbbell formation. At the initial stage of the dumbbell formation, the lobes are formed like a nucleation process, where small protrusions nucleate on the seed particle surface. When the polymerization occurs, the lobe grows and can mitigate along the surface to merge into bigger lobes. Eventually when the phase separation is complete, the dumbbell morphology dominates the system and the polymerization continues to grow the single lobe on the dumbbell.

However, when methanol-water ratio is high (6:1), seed particles will swell directly into dumbbell morphologies. No multilobe morphology is observed. The subsequent polymerization also preserves the dumbbell morphology.

3.3. Effect of crosslinking

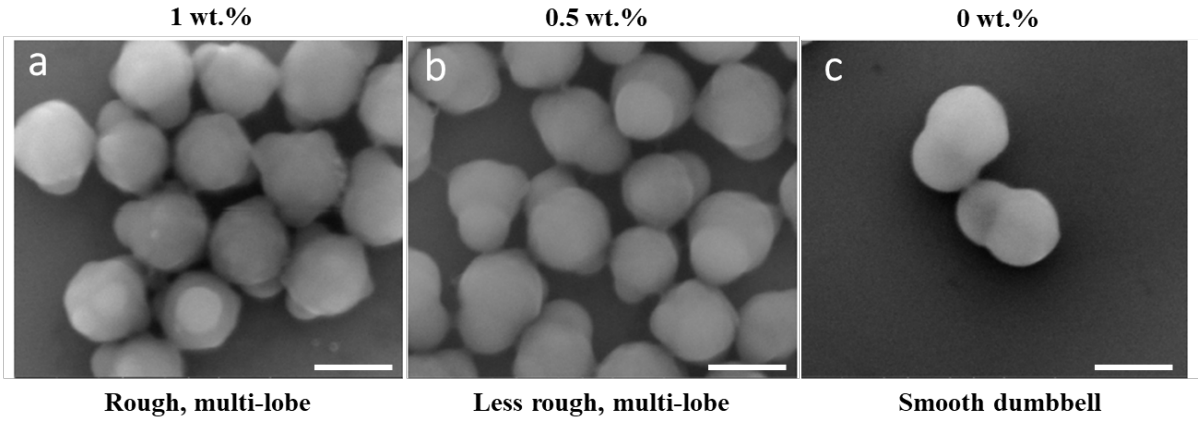

Fig. 5. Different particle morphologies (multilobe and single protrusion) formed by adding different crosslinker amount in the second polymerization: a) 1 wt.%; b) 0.5 wt.%, c) 0 wt.%. Scale bar: 500nm.

Fig. 5 shows the particle morphology when prepared with different amount of crosslinkers added with the second monomer. When the concentration of crosslinkers increases, the surface becomes rougher and particle morphology changes from dumbbell to multilobe. The phenomenon is consistent with our nucleation and growth model. Increasing crosslinker concentration will lead to higher viscosity and lower diffusion rate at the particle surface, which prevents the multilobes from merging efficiently into a single

lobe separation. Previous studies on the crosslinking density of the seed particles also showed similar trend [11].

3.4. Computer simulations of morphology evolution

3.4.1. Model validation

Based on the experimental results, we content that entanglements among crosslinked polymer chains have great impact on the mobility of polymers and thus affect the kinetics of the morphology evolution. In order to properly incorporate the entanglement effect, we calibrated the dynamic bond model by simulating melts of monodisperse polymers and measuring the diffusivity of individual chains. Linear crosslinking structures with different lengths were considered to enable a comparison against the reputation theory [62]. In particular, the total degree of polymerization of the chain was varied by the number of polymer beads that are linearly crosslinked. The reptation model predicts $D \sim N^{-\nu}$, where D is the chain diffusion coefficient and N is the length of linear polymers. The value of index ν equals 1 when no entanglements are considered and takes the value 2 with the entanglement effect [62]. **Fig. 6** shows that the simulations without dynamic bonds resulted in ν approximately equal to 1. This indicates that the highly coarse-grained model did not inherently capture topological constraints of long polymers and thus the polymer diffusion was unphysically enhanced. In contrast, $\nu = 2$ can be successfully obtained with the addition of dynamic bonds by setting appropriate coefficients of the Bell model (listed in SI). This comparison confirms the dynamic bonds allow our model to reproduce the correct dynamics of entangled chains. Using the validated entanglement model, we then simulated the seeded emulsion polymerization simulations of Janus particle synthesis. Below, the simulation results focus on the secondary monomer polymerization

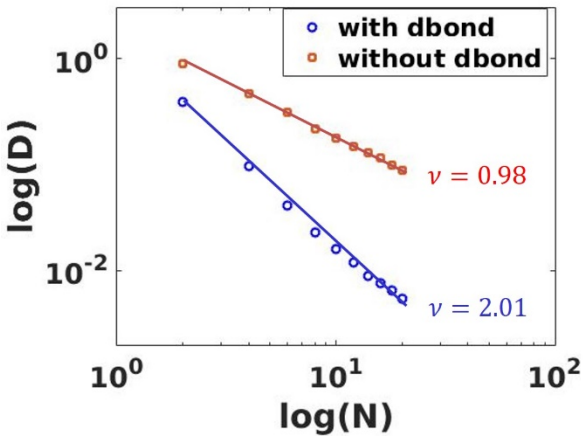

Fig. 6. The relation between chain diffusion coefficient and polymer length in linear polymer melts with and without the implementation of the dynamic bond model in DPD simulations.

3.4.2. Dynamic evolution from multilobe to dumbbell morphology

The morphology transition from multilobe to dumbbell was observed most saliently during the polymerization with seed synthesized under 4:1 methanol-water ratio and 0 wt.% DVB added with the second monomer. Despite no chemical crosslinker in the secondary monomer polymerization, polymer chains could still form physical crosslinks in the experimental system. Correspondingly, we simulated the polymerization for the seed particle and second polymer protrusions having low numerical degrees of crosslinking (30%) and explored morphology transition in great detail. **Fig. 7(a-d)** and **Video S1** show the dumbbell was progressively formed by the coalescence of small protrusions during the simulation. **Fig. 7e** shows the change in the relative shape anisotropy accompanied with the morphology development, in which the sudden increases correspond to the instants when the lobes merge. We also conducted independent runs with different initial bead distributions to confirm the consistency of this behavior, as shown in **Fig. 7f.** Moreover, another simulation having the seed and second polymers crosslinked at 10% also exhibited a similar behavior (**Fig. S5**), verifying the morphology transition at low crosslinking degree.

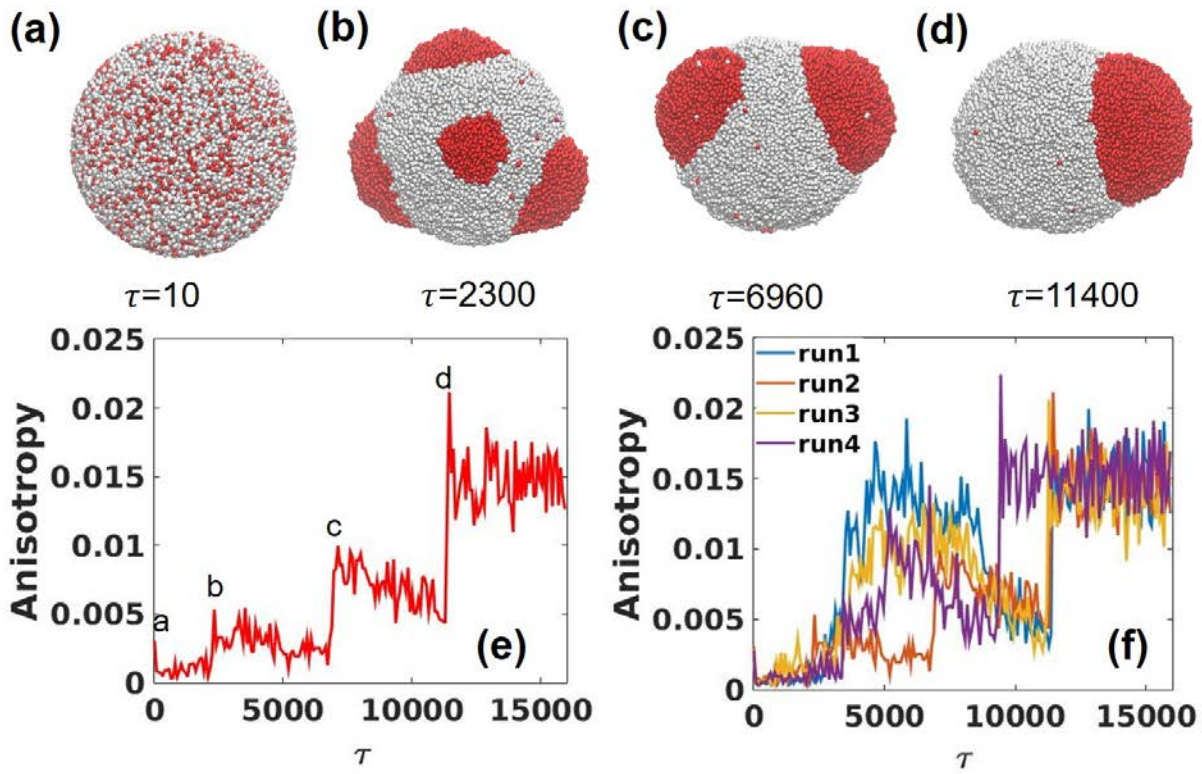

Fig. 7. (a)-(d) Dynamic change of particle morphology toward a Janus dumbbell at different time. The numerical crosslinking degrees of both seed particle and second polymers are 30% (note the numerical degree of crosslinking reflects in simulation does not reflect the actual crosslinking density). The white and red beads represent the seed polymers and second polymers, respectively. (e) The corresponding time-dependent relative shape anisotropy that reveals the morphology change of (a)-(d). (f) Relative shape anisotropy of independent runs with different initial configurations.

3.4.3. Seed crosslinking degree effect

To probe the effect of seed structure on the final particle morphology, we constructed seed particles with different crosslinking degrees from 0% to 90%. As mentioned in Section 2.5, this step-wise difference in the numerical degree of crosslinking reflects the similar trend as the particles obtained from experiment but does not reflect their actual crosslinking density. The number of crosslinkers in the second monomer was fixed to achieve 90% crosslinking degree of the second polymer at the end of simulation. **Fig. 8** shows that the lightly crosslinked seeds yielded dumbbell morphology, in which the second polymers

aggregated into a single protrusion. When the numerical degree of crosslinking in the seed increased, multiple lobes of second polymer were observed in the final morphology. The number of lobes increased with the degree of seed crosslinking and a maximum of 4 lobes was obtained for the 90% crosslinked seed. The interfaces between the seed-polymer-rich and second-polymer-rich domains were flat (see the insets of **Fig. 8**), which was attributed to the large surface tension between the seed and second polymers. Multilobe morphology clearly produces large interfacial area and was not thermodynamically favorable. **Fig. S6a** shows the relative shape anisotropy of Janus particle took a steady-state value at the end of simulation, suggesting a metastable state was reached. The comparison also shows that the final anisotropy value decreased as the seed crosslinking degree increased. This variation is consistent with the observed morphology change. These results verify that the crosslinking structure of the seed significantly influences the kinetics of morphology evolution. Therefore, highly crosslinked seeds can result in Janus particles in metastable states.

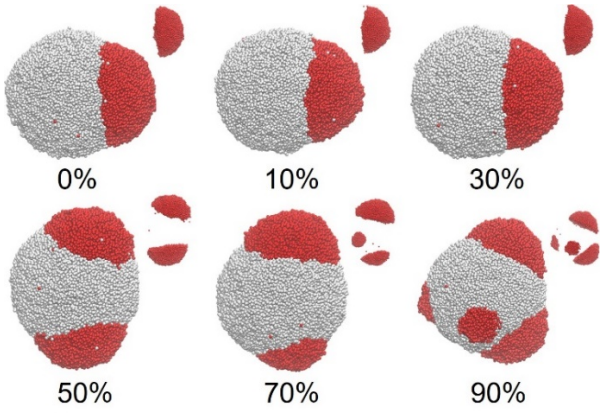

Fig. 8. Final morphologies of Janus particles in simulation for seed crosslinking degrees of 0%, 10%, 30%, 50%, 70%, and 90%. This step-wise difference bares the similar trend as the particles obtained from experiment but does not reflect their actual crosslinking density. The terminal crosslinking degree of second polymer is fixed at 90%. The insets show the morphologies of the second polymer lobes.

3.3.4. Effect of degree of crosslinking in second polymer

To complement our experimental observation, we also investigated the crosslinking effect of the second

polymers for two different seed particles that are 45% and 90% crosslinked. **Fig. 9a** shows that by increasing the numerical crosslinking degree of second polymers, the metastable morphology changed from dumbbell and multilobe for the 45% crosslinked seeds. With higher crosslinking degree in the seed, the twin lobe particle can be obtained even when the second monomer has maximum mobility with no numerical crosslinkers (**Fig. 9b**). The number of lobes further increased from 2 to 4 when the amount of second polymer crosslinkers increased. **Fig. S6b** also confirms these morphologies reached metastable states without any further development in the course of simulation.

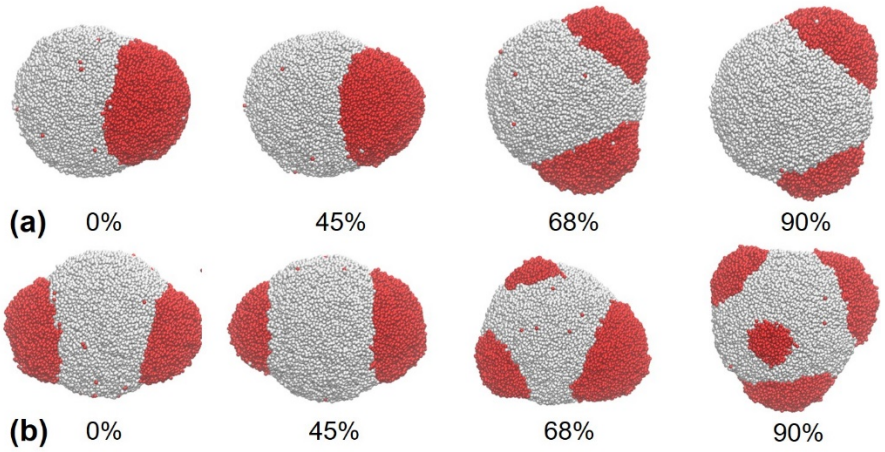

Fig. 9. Final morphologies of Janus particle in the simulations for the numerical crosslinking degrees of 0%, 45%, 68%, and 90% for the second polymer (note this step-wise difference in the numerical degree of crosslinking reflects the similar trend as the particles obtained from experiment but does not reflect their actual crosslinking density). Panels (a) and (b) show the results for the 45% and 90% crosslinked seeds, respectively.

Fig. 8 and **Fig. 9** confirm that the thermodynamically unfavorable multilobe morphologies are metastable states as a result of the small lobes being mechanically trapped in highly crosslinked seeds. In some simulations, we can observe small lobes of second polymer internally trapped in the seed particle, as shown in **Fig. S7**. Furthermore, the entanglements between the networks inhibit coalescence in the lobes. We conducted a computer experiment to explicitly elucidate the effect of entanglements on morphology

evolution. **Fig. S8** shows that the dynamic bond model is necessary to capture the kinetically trapped states as well as the multilobe morphology observed in the experiments. Detailed discussion of this computational experiment is given in SI.

3.5 Kinetic and thermodynamic mechanism

Previous studies suggested that the entire process of seeded emulsion polymerization and morphology formation can be attributed to three competitive driving forces. The first is the elastic force induced by the swelling of the crosslinked seed. The second is balancing the free energy of mixing the monomer with the polymeric seed. The third is the surface tension between particle surface and continuous phase interface [36]. This model is summarized by the following equation: $\Delta G_{m,p} = \Delta G_{el} + \Delta G_m + \Delta G_t$, where $\Delta G_{m,p}$ is the total free energy change, ΔG_{el} is the elastic energy change resulting from the crosslinked seed, ΔG_m is the free energy change from mixing of monomer and polymeric seed, which is determined by the Flory-Huggins parameters, and ΔG_t is the interfacial surface energy change between the particle and solvent. Due to the molecular weight and crosslinking density difference, different seed particles synthesized under different methanol-water ratios will have different Flory-Huggins parameters. This can partially account for the difference of swelling behaviors observed in experiment. However, since Flory-Huggins parameter only contributes to ΔG_m, which alone could not explain all the morphology changes observed in our study. In addition, the equation here can only predict the equilibrated state. Our observation focuses on the kinetics, which is more complicated. Notably, our coarse-grained simulations do not consider the variations of Flory-Huggins parameters but are capable of predicting particle morphology consistent with experimental data. This indicates different Flory-Huggins parameters may have only minor effects on the morphology development.

Nonetheless, this model points out the most important interactions in our system. The elastic force and free energy of mixing will induce the initial protrusion of monomers nucleated at different locations on seed particle surface, while the surface tension tends to minimize the surface area by forming a dumbbell morphology. At low methanol-water ratio (1:1), the seed particles are rougher with higher crosslinking

density. In this case, it is difficult for the protrusions to diffuse and merge. This eventually leads to the formation of multilobe morphology. When the methanol-water ratio increases (6:1), the seed particles become smooth and crosslinking density decreases. Thus, the mobility of initial protrusions increases, which promotes the formation of thermodynamically favored single protrusion (dumbbell morphology).

Evolution of particle morphology during the polymerization of the second monomer is governed by the merge and coalescing of initial protrusions induced by swelling. Thermodynamic equilibrium of this stage is dictated by the surface tension, where the internal elasticity of seed network and the free energy of partial mixing have negligible effects as the monomer is consumed away by polymerization. The morphology evolution again is kinetically controlled by the diffusion and viscoelastic behavior of the protrusions. The mobility and coalescence of the protrusions on the seed surface can be controlled by the amount of crosslinkers within the second monomers. More crosslinking will slow down the merge of lobes and eventually lead to kinetically trapped multilobe morphology.

4. Conclusions

In summary, we probe the kinetics of morphology formation in a multistage emulsion polymerization for achieving Janus dumbbell nanoparticles. Using integrated experimental and computational tools, we demonstrated that by simply adjusting the methanol concentration during seed synthesis, we can change the seed morphology from spherical to dumbbell shape. In addition, when the methanol amount was low, spherical seeds with rough surface were obtained, which further resulted in multilobe particle after the secondary monomer polymerization. When the methanol amount was high, spherical seed with smooth surface were obtained and produced Janus dumbbell nanoparticles after the secondary monomer polymerization. When the methanol amount was intermediate, the final particle morphology went through a multilobe to dumbbell transition during the secondary monomer polymerization. The study on the effect of crosslinking density further revealed that particle morphology changed from dumbbell shape to multilobe morphology when more crosslinker was added in the second monomer polymerization. Based on the results, a nucleation-growth model has been proposed. The final morphology is governed by the

interplay of thermodynamics equilibrium and mobility of protrusions on the seed particle surface. When the protrusions have chance to merge together, dumbbell morphology can be successfully obtained. Otherwise, the protrusions will be arrested kinetically and lead to multilobe morphology. The computer simulation further confirms that the morphology is kinetically controlled by diffusion of the protrusions on the seed particles. This study provides fundamental understanding of morphology formation kinetics during a seeded emulsion polymerization and offers guidance for future scale-up synthesis and morphology control of polymeric Janus nanoparticles.

Acknowledgement: The experiment part of this work was supported by Iowa State University Start-up Fund, Regents Innovation Fund and 3M Nontenured Faculty Award. The simulation part of this work was partially supported by the American Chemical Society Petroleum Research Fund under grant No. 56884-DNI9 and used resources of the Center for Functional Nanomaterials, which is a U.S. DOE Office of Science Facility, at Brookhaven National Laboratory under contract no. DE-SC0012704.

References

[1] K.L. Chen, S.X. Zhou, S. Yang, L.M. Wu, Advanced Functional Materials 25(7) (2015) 1035-1041.

[2] J. Gaitzsch, X. Huang, B. Voit, Chem Rev 116(3) (2016) 1053-93.

[3] C. Kaewsaneha, P. Tangboriboonrat, D. Polpanich, M. Eissa, A. Elaissari, Colloids and Surfaces a-Physicochemical and Engineering Aspects 439 (2013) 35-42.

[4] B.T.T. Pham, C.H. Such, B.S. Hawkett, Polymer Chemistry 6(3) (2015) 426-435.

[5] K. Yoon, D. Lee, J.W. Kim, J. Kim, D.A. Weitz, Chem Commun (Camb) 48(72) (2012) 9056-8.

[6] C. Kang, A. Honciuc, ACS Nano 12(4) (2018) 3741-3750.

[7] F. Liang, B. Liu, Z. Cao, Z. Yang, Langmuir 34(14) (2018) 4123-4131.

[8] J. Zhang, B.A. Grzybowski, S. Granick, Langmuir 33(28) (2017) 6964-6977.

[9] C. Kang, A. Honciuc, J Phys Chem Lett 9(6) (2018) 1415-1421.

[10] B.G.P. van Ravensteijn, W.K. Kegel, J Colloid Interface Sci 490 (2017) 462-477.

[11] B. Peng, H.R. Vutukuri, A. van Blaaderen, A. Imhof, Journal of Materials Chemistry 22(41) (2012) 21893-21900.

[12] W.H. Chen, F.Q. Tu, L.C. Bradley, D. Lee, Chemistry of Materials 29(7) (2017) 2685-2688.

[13] W.C. Yan, M.W. Pan, J.F. Yuan, G. Liu, L.X. Cui, G.L. Zhang, L. Zhu, Polymer 122 (2017) 139-147.

[14] C. Li, Z. Wu, Y.F. He, P.F. Song, W. Zhai, R.M. Wang, J Colloid Interface Sci 426 (2014) 39-43.

[15] S. Jiang, A. Van Dyk, A. Maurice, J. Bohling, D. Fasano, S. Brownell, Chem Soc Rev 46(12) (2017) 3792-3807.

[16] S. Jiang, Q. Chen, M. Tripathy, E. Luijten, K.S. Schweizer, S. Granick, Adv Mater 22(10) (2010) 1060-71.

[17] B. Mizrahi, X. Khoo, H.H. Chiang, K.J. Sher, R.G. Feldman, J.J. Lee, S. Irusta, D.S. Kohane, Langmuir 29(32) (2013) 10087-94.

[18] M.S. Yavuz, F. Buyukserin, Z. Zengin, S.T. Camli, Journal of Polymer Science Part a-Polymer Chemistry 49(22) (2011) 4800-4808.

[19] Y. Ma, W.F. Dong, M.A. Hempenius, H. Mohwald, G.J. Vancso, Nat Mater 5(9) (2006) 724-9.

[20] F. Tu, B.J. Park, D. Lee, Langmuir 29(41) (2013) 12679-87.

[21] D.O. Grigoriev, K. Köhler, E. Skorb, D.G. Shchukin, H. Möhwald, Soft Matter 5(7) (2009).

[22] L. Liao, J. Liu, E.C. Dreaden, S.W. Morton, K.E. Shopsowitz, P.T. Hammond, J.A. Johnson, J Am Chem Soc 136(16) (2014) 5896-9.

[23] N. Korin, M. Kanapathipillai, B.D. Matthews, M. Crescente, A. Brill, T. Mammoto, K. Ghosh, S. Jurek, S.A. Bencherif, D. Bhatta, A.U. Coskun, C.L. Feldman, D.D. Wagner, D.E. Ingber, Science 337(6095) (2012) 738-42.

[24] Y. Jiang, T.I. Löbling, C. Huang, Z. Sun, A.H.E. Müller, T.P. Russell, ACS Applied Materials & Interfaces 9(38) (2017) 33327-33332.

[25] C. Tang, C. Zhang, J. Liu, X. Qu, J. Li, Z. Yang, Macromolecules 43(11) (2010) 5114-5120.

[26] J.G. Park, J.D. Forster, E.R. Dufresne, J Am Chem Soc 132(17) (2010) 5960-1.

[27] D. Nagao, M. Hashimoto, K. Hayasaka, M. Konno, J Macromolecular Rapid Communications 29(17) (2008) 1484-1488.

[28] Y. Liu, Q. Yang, J. Zhu, L. Liu, W. Yang, J Colloid Polymer Science 293(2) (2015) 523-532.

[29] B. Liu, J. Liu, F. Liang, Q. Wang, C. Zhang, X. Qu, J. Li, D. Qiu, Z. Yang, Macromolecules 45(12) (2012) 5176-5184.

[30] Y. Sun, F. Liang, X. Qu, Q. Wang, Z. Yang, Macromolecules 48(8) (2015) 2715-2722.

[31] J.W. Kim, R.J. Larsen, D.A. Weitz, J Am Chem Soc 128(44) (2006) 14374-7.

[32] D. Wu, J.W. Chew, A. Honciuc, Langmuir 32(25) (2016) 6376-86.

[33] Y. Liu, W. Liu, Y. Ma, L. Liu, W. Yang, Langmuir 31(3) (2015) 925-936.

[34] X. Fan, J. Yang, X.J. Loh, Z. Li, Macromolecular Rapid Communications 0(0) (2018) 1800203.

[35] Q. Peng, H. Cong, B. Yu, L. Wei, K. Mahmood, H. Yuan, R. Yang, X. Zhang, Y. Wu, Journal of Colloid and Interface Science 522 (2018) 144-150.

[36] E.B. Mock, H. De Bruyn, B.S. Hawkett, R.G. Gilbert, C.F. Zukoski, Langmuir 22(9) (2006) 4037-43.

[37] J.-B. Fan, H. Liu, Y. Song, Z. Luo, Z. Lu, S. Wang, Macromolecules 51(5) (2018) 1591-1597.

[38] F. Tu, D. Lee, J Am Chem Soc 136(28) (2014) 9999-10006.

[39] C.X. Wei, A. Plucinski, S. Nuasaen, A. Tripathi, P. Tangboriboonrat, K. Tauer, Macromolecules 50(1) (2017) 349-363.

[40] Y.-S. Cho, S.-H. Kim, J.H.J.K.J.o.C.E. Moon, 29(8) (2012) 1102-1107.

[41] Y. Reyes, J.M. Asua, 48(12) (2010) 2579-2583.

[42] Y. Duda, F. Vazquez, Langmuir 21(3) (2005) 1096-102.

[43] Y.G. Durant, D.C. Sundberg, 58(9) (1995) 1607-1618.

[44] O.J. Karlsson, J.M. Stubbs, R.H. Carrier, D.C. Sundberg, Polymer Reaction Engineering 11(4) (2003) 589-625.

[45] J.M. Stubbs, R. Carrier, O.J. Karlsson, D.C. Sundberg, Simulation of particle morphology development under kinetically controlled conditions, Springer Berlin Heidelberg, Berlin, Heidelberg, 2004, pp. 131-137.

[46] J. Stubbs, R. Carrier, D.C. Sundberg, 17(4 - 5) (2008) 147-162.

[47] E. Akhmatskaya, J.M. Asua, J Polym Sci Pol Chem 50(7) (2012) 1383-1393.

[48] E. Akhmatskaya, J.M. Asua, Colloid and Polymer Science 291(1) (2013) 87-98.

[49] S. Hamzehlou, J.R. Leiza, J.M. Asua, Chem Eng J 304 (2016) 655-666.

[50] P.J. Hoogerbrugge, J.M.V.A. Koelman, Europhys Lett 19(3) (1992) 155-160.

[51] P. Espanol, P. Warren, Europhys Lett 30(4) (1995) 191-196.

[52] R.D. Groot, P.B. Warren, Journal of Chemical Physics 107(11) (1997) 4423-4435.

[53] X. Yong, O. Kuksenok, A.C. Balazs, Polymer 72 (2015) 217-225.

[54] X. Yong, 8(12) (2016) 426.

[55] S. Chen, X. Yong, J Chem Phys 149(9) (2018) 094904.

[56] G.I. Bell, Science 200(4342) (1978) 618-27.

[57] B.V.S. Iyer, I.G. Salib, V.V. Yashin, T. Kowalewski, K. Matyjaszewski, A.C. Balazs, Soft Matter 9(1) (2013) 109-121.

[58] G. Xu, Z. Huang, P. Chen, T. Cui, X. Zhang, B. Miao, L.-T. Yan, 13(13) (2017) 1603155.

[59] H.R. Sheu, M.S. El-Aasser, J.W. Vanderhoff, Journal of Polymer Science Part A: Polymer Chemistry 28(3) (1990) 653-667.

[60] J.-W. Kim, K.-D. Suh, Polymer 41(16) (2000) 6181-6188.

[61] Y. Liu, Y. Ma, L. Liu, W. Yang, Journal of Colloid and Interface Science 445 (2015) 268-276.

[62] P.G.d. Gennes, The Journal of Chemical Physics 55(2) (1971) 572-579.